Redetermination of metarossite, $CaV^{5+}_2O_6 \cdot 2H_2O$

Anaïs Kobsch,[a,b]* Robert T. Downs[c] and Kenneth J. Domanik[d]

[a]Département des Sciences de la Terre, École Normale Supérieure de Lyon, Site Monod, 15 parvis René Descartes, BP 7000, 69342 Lyon, France, [b]Département des Sciences de la Terre, Université Claude Bernard Lyon 1, 43 Bd du 11 Novembre 1918, 69622 Villeurbanne Cedex, France, [c]Department of Geosciences, University of Arizona, 1040 E. 4th Street, Tucson, AZ 85721-0077, USA, and [d]Lunar and Planetary Laboratory, University of Arizona, 1629 E. University Blv, Tucson, AZ 85721-0092, USA. *Correspondence e-mail: anais.kobsch@ens-lyon.fr

The crystal structure of metarossite, ideally $CaV_2O_6 \cdot 2H_2O$ [chemical name: calcium divanadium(V) hexaoxide dihydrate], was first determined using precession photographs, with fixed isotropic displacement parameters and without locating the positions of the H atoms, leading to a reliability factor $R = 0.11$ [Kelsey & Barnes (1960). *Can. Mineral.* **6**, 448–466]. This communication reports a structure redetermination of this mineral on the basis of single-crystal X-ray diffraction data of a natural sample from the Blue Cap mine, San Juan County, Utah, USA ($R1 = 0.036$). Our study not only confirms the structural topology reported in the previous study, but also makes possible the refinement of all non-H atoms with anisotropic displacement parameters and all H atoms located. The metarossite structure is characterized by chains of edge-sharing $[CaO_8]$ polyhedra parallel to [100] that are themselves connected by chains of alternating $[VO_5]$ trigonal bipyramids parallel to [010]. The two H_2O molecules are bonded to Ca. Analysis of the displacement parameters show that the $[VO_5]$ chains librate around [010]. In addition, we measured the Raman spectrum of metarossite and compared it with IR and Raman data previously reported. Moreover, heating of metarossite led to a loss of water, which results in a transformation to the brannerite-type structure, CaV_2O_6, implying a possible dehydration pathway for the compounds $M^{2+}V_2O_6 \cdot xH_2O$, with M = Cu, Cd, Mg or Mn, and x = 2 or 4.

1. Mineralogical and crystal-chemical context

Metarossite was originally described from Bull Pen Canyon, San Miguel County, Colorado, by Foshag & Hess (1927) as a yellow, platy, soft and friable mineral with composition $CaV_2O_6 \cdot 2H_2O$. It is soluble in hot water and generally is formed as a dehydration product of rossite, $CaV_2O_6 \cdot 4H_2O$, which itself crystallizes from aqueous solutions (Ahmed & Barnes, 1963).

Barnes & Qurashi (1952) reported triclinic symmetry ($P\bar{1}$) and unit-cell parameters [a = 6.215 (5), b = 7.065 (5), c = 7.769 (5) Å, α = 92.97 (17), β = 96.65 (17), γ = 105.78 (17)°] of metarossite from a sample from an area near Thompson's, Utah. Later, by means of precession photographs, Kelsey & Barnes (1960) determined its crystal structure from the material used by Barnes & Qurashi (1952). For structure refinement (R = 0.11), fixed isotropic displacement parameters were introduced without locating the positions of the hydrogen atoms.

This study reports the refinement of the structure of a metarossite sample (Fig. 1) from the Blue Cap mine, San Juan County, Utah, USA, with anisotropic displacement para-

R100065   500 µm

Table 1
Hydrogen-bond geometry (Å, °).

$D—H\cdots A$	$D—H$	$H\cdots A$	$D\cdots A$	$D—H\cdots A$
$OW3—H1\cdots O4^{i}$	0.78 (5)	2.37 (5)	2.965 (4)	133 (4)
$OW3—H2\cdots O5^{ii}$	0.72 (4)	2.25 (5)	2.900 (3)	150 (5)
$OW8—H3\cdots O5^{iii}$	0.75 (4)	2.09 (5)	2.810 (3)	162 (5)
$OW8—H4\cdots O5^{iv}$	0.84 (4)	1.97 (5)	2.794 (3)	166 (4)

Symmetry codes: (i) $-x + 1, -y + 1, -z + 1$; (ii) $x + 1, y + 1, z$; (iii) $x, y + 1, z$; (iv) $-x, -y + 1, -z$.

Figure 1
Photograph of the metarossite specimen analyzed in this study.

meters for all non-hydrogen atoms, positions of hydrogen atoms determined, and improvement of the reliability factor to 0.036. Raman spectra were also recorded and compared with that reported in the two studies by Frost *et al.* (2004, 2005), on a sample from the Burro mine, San Miguel County of Colorado, USA.

2. Structural commentary

The structural topology of metarossite for all non-hydrogen atoms from this study is identical to that reported by Kelsey & Barnes (1960). Chains of edge-sharing distorted [VO$_5$] trigonal bipyramids run parallel to [010], with [V1O$_5$] and [V2O$_5$] polyhedra alternating along the chains (Fig. 2a). These chains are linked by chains of edge-sharing [CaO$_8$] polyhedra aligned parallel to [100] (Fig. 2b). The water molecules are located at three vertices of the [CaO$_8$] polyhedra [OW3, OW8^{i} and OW8^{ii}; symmetry codes: (i) $-x + 1, -y + 1, -z$; (ii) $x + 1, y, z$].

It is interesting to note that there is a radial orientation of the displacement ellipsoids associated with the [VO$_5$] chains when viewed along the chain direction (Fig. 3). The amplitude also slightly radially increases, as indicated by the black dashed circles in Fig. 3. We interpret this as the oscillation or libration of the [VO$_5$] chains around [010]. A similar behavior was reported for brackebuschite Pb$_2$Mn^{3+}(VO$_4$)$_2$(OH) (Lafuente & Downs, 2016) where the [Mn^{3+}(VO$_4$)$_2$OH] chains oscillating about an axis.

Numerical data of the hydrogen-bonding scheme in metarossite are presented in Table 1. The bond-valence calculations (Brown, 2002) with the parameters given by Brese & O'Keeffe (1991) confirm that OW3 and OW8 correspond to the two H$_2$O molecules (Table 2). The low bond-valence sum for O5 is because it is an acceptor for three hydrogen atoms (H2, H3 and H4; Table 1). In fact, all acceptor O atoms involved in hydrogen bonding are from VO$_5$ polyhedra,

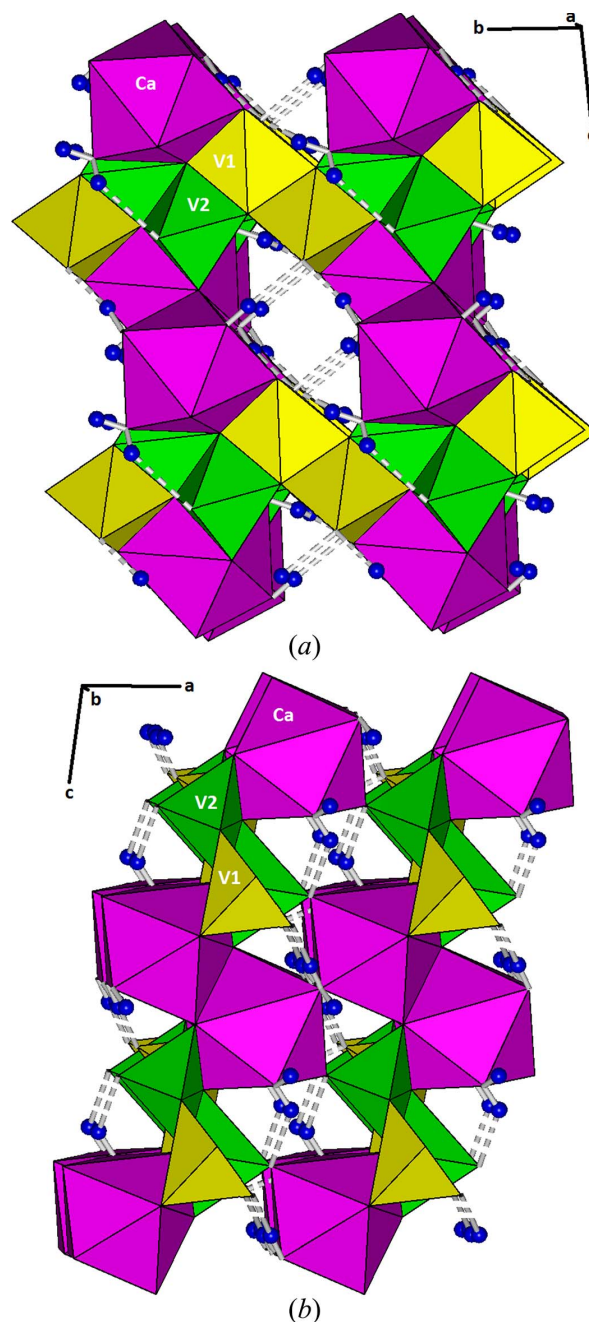**Figure 2**
Crystal structure of metarossite, showing (a) the chains of alternating [V1O$_5$] and [V2O$_5$] trigonal bipyramids (yellow and green, respectively) along [010], and (b) the chains of edge-sharing distorted [CaO$_8$] square antiprisms (magenta) along [100]. H atoms are represented by blue spheres; hydrogen bonding is indicated by dashed lines.

Table 2
Bond-valence sums for metarossite.

	O1	O2	OW3*	O4	O5	O6	O7	OW8*	Σ_M
Ca		0.253	0.218	0.315		0.272	0.240	0.205	**2.107**
							0.326	0.278	
V1	0.581	0.687			1.491	1.624			**5.153**
	0.770								
V2	0.825	0.780		1.584			1.415		**5.083**
		0.479							
Σ_O	**2.176**	**2.200**	**0.218**	**1.899**	**1.491**	**1.897**	**1.981**	**0.482**	

Note: (*) H atoms not considered for calculation.

Table 3
O···O measured distances (Å), Raman stretching frequencies (cm^{-1}) calculated using the correlation for $d < 3.2$ Å and samples without Cu (Libowitzky, 1999), and comparison with O···O calculated by Frost et al. (2004) from IR frequencies (cm^{-1})..

	This study		Frost et al. (2004)	
O—H···O	O···O	ν	ν	O···O
OW3—H1···O4	2.965	3504	3526	2.9393
OW3—H2···O5	2.900	3482	3387	2.7995
OW8—H3···O5	2.810	3421	3181	2.6977
OW8—H4···O5	2.794	3404	2867	2.6227

providing the additional linkage between the [CaO$_8$] and [VO$_5$] chains.

3. Raman spectrum

The Raman spectrum of metarossite (Fig. 4) is comparable with the data recorded by Frost et al. (2005) below 1000 cm^{-1}, but is different in the O–H stretching region between 2800 and 3700 cm^{-1} (Frost et al., 2004). Indeed, they recorded only three Raman bands (at 3177, 3401 and 3473 cm^{-1}), whereas with the present data, it is possible to distinguish four to five bands depending on the orientation (2904, 2954, 3189, 3240 and 3398 cm^{-1}), along with a broad shoulder around 3415–3480 cm^{-1} (Fig. 4). According to Libowitzky (1999), the band at 3398 cm^{-1} can be attributed to the OW8–H4 vibration, and the broad shoulder around 3415–3480 cm^{-1} may correspond to the OW8–H3 and OW3–H2 vibrations (Table 3). The last vibration (OW3–H1) cannot be seen on Fig. 4, but since the
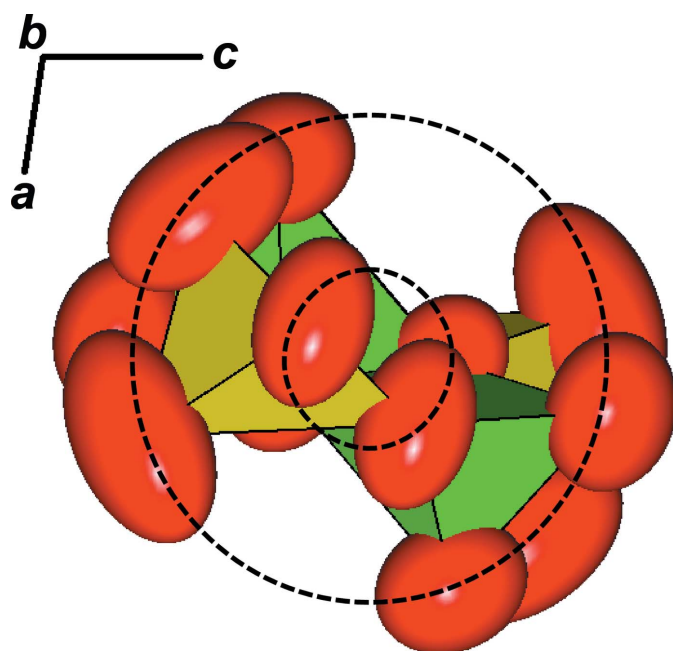
frequency currently accepted for free OH$^-$ ion is 3560 cm^{-1} (Lutz, 1995), it can be associated with the IR band at 3526 cm^{-1} observed by Frost et al. (2004).

4. Synthesis and crystallization

The natural sample used in this study is from the Blue Cap mine, San Juan County of Utah, USA (Fig. 1) and belongs to the RRUFF project collection (http://rruff.info/R100065). Chemical analysis was performed with a CAMECA SX100 electron microprobe operated at 20 kV and 20 nA and a beam size <1 μm. Eight analysis points yielded an average composition (wt.%): CaO 19.2 (1), V$_2$O$_5$ 66.6 (4), trace amount of Sr, and H$_2$O 13.06 estimated to provide two H$_2$O molecules per formula unit. The empirical chemical formula, based on eight oxygen atoms, is Ca$_{0.94}$V$^{5+}_{2.02}$O$_6$·2H$_2$O. The Raman spectrum of metarossite was collected from a randomly oriented crystal at 50% power of 150 mW on a Thermo–Almega microRaman system, using a solid-state laser with a wavelength of 532 nm and a thermoelectrically cooled CCD detector. The laser was

Figure 3
A view down [010] of the [VO$_5$] chain composed of alternated [V1O$_5$] (yellow) and [V2O$_5$] (green) polyhedra. The red ellipsoids represent the displacement parameters of the O atoms at the 99.999% probability level. The black circles demonstrate that the entire [VO$_5$] chain oscillate or librate around [010], with a slight radial increase of amplitudes.
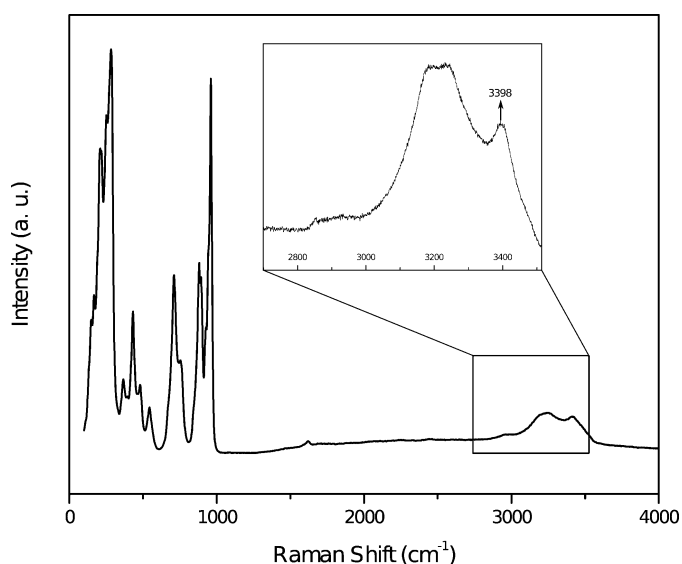

Figure 4
Raman spectrum of metarossite collected with a 532 nm laser. Only the band at 3400 cm^{-1} can be clearly assigned to hydrogen stretching vibrations (OW8–H4) but the broad shoulder discernible around 3415–3480 cm^{-1} corresponds probably to OW8–H3 and OW3–H2 vibrations.
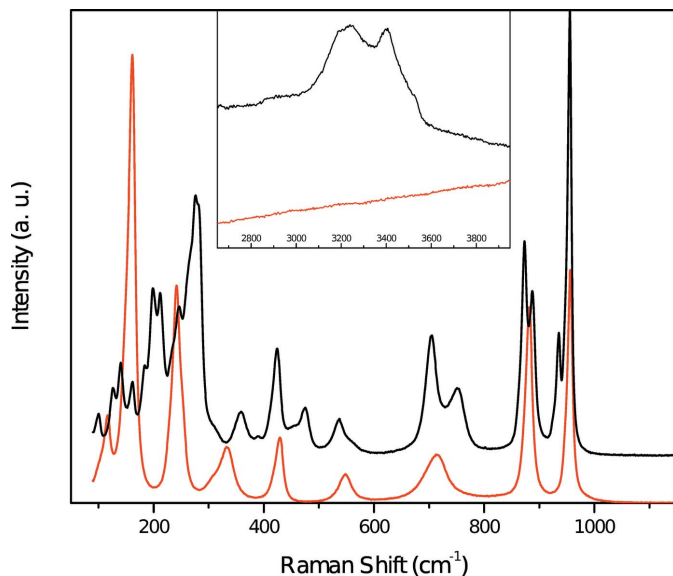
Figure 5
Raman spectrum of metarossite after heated by a full power 532 nm laser (red curve) and comparison with an initial metarossite spectrum (black curve).

partially polarized with 4 cm^{-1} resolution and a spot size of 1 μm.

5. Transformation of metarossite

When a small piece of metarossite (edge length in all dimensions 0.1 mm) was placed under a full power laser (150 mW, 532 nm), a change in its Raman spectrum was observed (Fig. 5). In particular, all bands originating from O–H stretching vibrations disappeared, suggesting a complete dehydration of the sample. Moreover, the spectrum below 1200 cm^{-1} was found to match that of synthetic CaV$_2$O$_6$ (Baran *et al.*, 1987). In addition, we observed similar Raman spectra collected from a metarossite fragment that was heated in air in an oven at 373 K for 12 h. Single crystal X-ray diffraction analysis on the heated crystal revealed monoclinic symmetry with unit cell parameters $a = 10.0$ (1), $b = 3.6$ (2), $c = 6.9$ (6) Å, $\beta = 105$ (6)°, which match those reported for brannerite (Szymanski & Scott, 1982). However, we were unable to obtain more detailed structure information for the heated sample due to its poor crystallinity (caused probably by dehydration).

A number of synthetic metavanadates, such as those with formula M^{2+}V$_2$O$_6$ where M = Cu, Cd, Mg or Mn, are found to be isostructural with brannerite (Baran *et al.*, 1987; Müller-Buschbaum & Kobel, 1991). There are also many hydrated forms of these compounds, including synthetic CuV$_2$O$_6$·2H$_2$O (Leblanc & Ferey, 1990), and CdV$_2$O$_6$·2H$_2$O (Ulická, 1988), as well as natural dickthomssenite MgV$_2$O$_6$·7H$_2$O (Hughes *et al.*, 2001) or ansermetite MnV$_2$O$_6$·4H$_2$O (Brugger *et al.*, 2003). Because tetrahydrated or dihydrated forms of these materials have structures related to rossite or metarossite, it is likely, then, that natural equivalents of the synthetic metavanadates

Table 4
Experimental details.

Crystal data	
Chemical formula	CaV$_2$O$_6$·2H$_2$O
M_r	273.99
Crystal system, space group	Triclinic, $P\bar{1}$
Temperature (K)	293
a, b, c (Å)	6.2059 (4), 7.0635 (4), 7.7516 (5)
α, β, γ (°)	93.166 (4), 96.548 (4), 105.883 (4)
V (Å^3)	323.36 (4)
Z	2
Radiation type	Mo $K\alpha$
μ (mm^{-1})	3.68
Crystal size (mm)	0.07 × 0.07 × 0.06
Data collection	
Diffractometer	Bruker APEXII CCD area-detector
Absorption correction	Multi-scan (*SADABS*; Bruker, 2004)
T_{min}, T_{max}	0.669, 0.746
No. of measured, independent and observed [$I > 2\sigma(I)$] reflections	5576, 2075, 1508
R_{int}	0.037
$(\sin\theta/\lambda)_{max}$ (Å^{-1})	0.735
Refinement	
$R[F^2 > 2\sigma(F^2)]$, $wR(F^2)$, S	0.036, 0.076, 1.01
No. of reflections	2075
No. of parameters	113
H-atom treatment	Only H-atom coordinates refined
$\Delta\rho_{max}$, $\Delta\rho_{min}$ (e Å^{-3})	0.77, −0.58

Computer programs: *APEX2* and *SAINT* (Bruker, 2004), *SHELXT* (Sheldrick, 2015a), *SHELXL2014* (Sheldrick, 2015b), *XtalDraw* (Downs & Hall-Wallace, 2003) and *publCIF* (Westrip, 2010).

M^{2+}V$_2$O$_6$·xH$_2$O (M = Cu, Cd, Mg or Mn and x = 0, 2 or 4) may exist.

6. Refinement details

Crystal data, data collection and structure refinement details are summarized in Table 4. The electron microprobe analysis revealed traces of Sr in our sample. The empirical formula shows a little deficiency for Ca and excess for V. For simplicity, the ideal chemical formula CaV$_2$O$_6$·2H$_2$O was assumed during the refinement. Kelsey & Barnes (1960) underline that {101} is often a twin-plane in metarossite, but the crystal used for this X-ray analysis did not show twinning. Atomic coordinates of the previous study were taken as starting parameters for refinement. The H atoms were located from difference Fourier syntheses and their positions refined with fixed isotropic displacement parameters ($U_{iso} = 0.04$ Å^2). The maximum residual electron density in the difference Fourier maps was located at 0.86 Å from O7 and the minimum density at 1.39 Å from Ca.

Acknowledgements

research communications

References

Ahmed, F. R. & Barnes, W. H. (1963). *Can. Mineral.* **7**, 713–726.
Baran, E. J., Cabello, C. I. & Nord, A. G. (1987). *J. Raman Spectrosc.* **18**, 405–407.
Barnes, W. H. & Qurashi, M. M. (1952). *Am. Mineral.* **37**, 407–422.
Brese, N. E. & O'Keeffe, M. (1991). *Acta Cryst.* **B47**, 192–197.
Brown, I. D. (2002). In *The Chemical Bond in Inorganic Chemistry: The Bond Valence Model.* Oxford University Press.
Brugger, J., Berlepsch, P., Meisser, N. & Armbruster, T. (2003). *Can. Mineral.* **41**, 1423–1431.
Bruker (2004). *APEX2, SAINT* and *SADABS.* Bruker AXS Inc., Madison, Wisconsin, USA.
Downs, R. T. & Hall-Wallace, M. (2003). *Am. Mineral.* **88**, 247–250.
Foshag, W. F. & Hess, F. L. (1927). *Proc. US Natl Museum*, **72**, 1–12.
Frost, R. L., Erickson, K. L. & Weier, M. L. (2004). *Spectrochim. Acta A Mol. Biomol. Spectrosc.* **60**, 2419–2423.
Frost, R. L., Erickson, K. L., Weier, M. L. & Carmody, O. (2005). *Spectrochim. Acta A Mol. Biomol. Spectrosc.* **61**, 829–834.
Hughes, J. M., Cureton, F. E., Marty, J., Gault, R. A., Gunter, M. E., Campana, C. F., Rakovan, J., Sommer, A. & Brueseke, M. E. (2001). *Can. Mineral.* **39**, 1691–1700.
Kelsey, C. H. & Barnes, W. H. (1960). *Can. Mineral.* **6**, 448–466.
Lafuente, B. & Downs, R. T. (2016). *Acta Cryst.* E**72**, 293–296.
Leblanc, M. & Ferey, G. (1990). *Acta Cryst.* C**46**, 15–18.
Libowitzky, E. (1999). *Monatsh. Chem.* **130**, 1047–1059.
Lutz, H. D. (1995). *Struct. Bond.* **82**, 85–103.
Müller-Buschbaum, H. & Kobel, M. (1991). *J. Alloys Compd.* **176**, 39–46.
Sheldrick, G. M. (2015a). *Acta Cryst.* A**71**, 3–8.
Sheldrick, G. M. (2015b). *Acta Cryst.* C**71**, 3–8.
Szymanski, J. T. & Scott, J. D. (1982). *Can. Mineral.* **20**, 271–279.
Ulická, Ľ. (1988). *Chem. Pap.* **42**, 11–19.
Westrip, S. P. (2010). *J. Appl. Cryst.* **43**, 920–925.

Redetermination of metarossite, $CaV^{5+}_2O_6 \cdot 2H_2O$

Anaïs Kobsch, Robert T. Downs and Kenneth J. Domanik

Computing details

Data collection: *APEX2* (Bruker, 2004); cell refinement: *SAINT* (Bruker, 2004); data reduction: *SAINT* (Bruker, 2004); program(s) used to solve structure: SHELXT (Sheldrick, 2015a); program(s) used to refine structure: *SHELXL2014* (Sheldrick, 2015b); molecular graphics: *XtalDraw* (Downs & Hall-Wallace, 2003); software used to prepare material for publication: *publCIF* (Westrip, 2010).

Calcium vanadium (V) oxide dihydrate

Crystal data

$CaV_2O_6 \cdot 2H_2O$	$Z = 2$
$M_r = 273.99$	$F(000) = 268$
Triclinic, $P\bar{1}$	$D_x = 2.814$ Mg m^{-3}
$a = 6.2059$ (4) Å	Mo $K\alpha$ radiation, $\lambda = 0.71073$ Å
$b = 7.0635$ (4) Å	Cell parameters from 1255 reflections
$c = 7.7516$ (5) Å	$\theta = 2.7$–29.8°
$\alpha = 93.166$ (4)°	$\mu = 3.68$ mm^{-1}
$\beta = 96.548$ (4)°	$T = 293$ K
$\gamma = 105.883$ (4)°	Platy, pale yellow
$V = 323.36$ (4) Å^3	$0.07 \times 0.07 \times 0.06$ mm

Data collection

Bruker APEXII CCD area-detector diffractometer	2075 independent reflections
	1508 reflections with $I > 2\sigma(I)$
φ and ω scan	$R_{int} = 0.037$
Absorption correction: multi-scan (*SADABS*; Bruker, 2004)	$\theta_{max} = 31.5°$, $\theta_{min} = 2.7°$
	$h = -9 \rightarrow 8$
$T_{min} = 0.669$, $T_{max} = 0.746$	$k = -10 \rightarrow 10$
5576 measured reflections	$l = -11 \rightarrow 11$

Refinement

Refinement on F^2	$w = 1/[\sigma^2(F_o^2) + (0.0318P)^2 + 0.0696P]$
Least-squares matrix: full	where $P = (F_o^2 + 2F_c^2)/3$
$R[F^2 > 2\sigma(F^2)] = 0.036$	$(\Delta/\sigma)_{max} < 0.001$
$wR(F^2) = 0.076$	$\Delta\rho_{max} = 0.77$ e Å^{-3}
$S = 1.01$	$\Delta\rho_{min} = -0.58$ e Å^{-3}
2075 reflections	Extinction correction: SHELXL2014
113 parameters	(Sheldrick, 2015b),
0 restraints	Fc*=kFc[1+0.001xFc$^2\lambda^3$/sin(2θ)]$^{-1/4}$
Hydrogen site location: difference Fourier map	Extinction coefficient: 0.005 (2)
Only H-atom coordinates refined	

Special details

Geometry. All esds (except the esd in the dihedral angle between two l.s. planes) are estimated using the full covariance matrix. The cell esds are taken into account individually in the estimation of esds in distances, angles and torsion angles; correlations between esds in cell parameters are only used when they are defined by crystal symmetry. An approximate (isotropic) treatment of cell esds is used for estimating esds involving l.s. planes.

Fractional atomic coordinates and isotropic or equivalent isotropic displacement parameters (Å^2)

	x	y	z	U_{iso}*/U_{eq}
Ca	0.76199 (10)	0.46286 (9)	0.14933 (8)	0.01285 (14)
V1	0.44824 (9)	0.10219 (7)	0.33438 (6)	0.01068 (13)
V2	0.37329 (8)	0.58264 (7)	0.34629 (6)	0.01004 (13)
O1	0.4051 (4)	0.8480 (3)	0.4170 (3)	0.0137 (4)
O2	0.5250 (3)	0.3869 (3)	0.3867 (3)	0.0106 (4)
OW3	0.8519 (5)	0.7632 (4)	0.3671 (4)	0.0236 (6)
O4	0.1030 (3)	0.4726 (3)	0.3330 (3)	0.0157 (5)
O5	0.1896 (4)	0.0684 (3)	0.2322 (3)	0.0207 (5)
O6	0.6214 (4)	0.1115 (3)	0.1910 (3)	0.0232 (5)
O7	0.4308 (4)	0.5998 (3)	0.1408 (3)	0.0155 (5)
OW8	0.0045 (4)	0.7225 (3)	0.0059 (3)	0.0164 (5)
H1	0.937 (8)	0.747 (6)	0.444 (6)	0.040*
H2	0.900 (8)	0.856 (7)	0.332 (6)	0.040*
H3	0.078 (8)	0.808 (7)	0.066 (6)	0.040*
H4	−0.069 (7)	0.766 (6)	−0.073 (6)	0.040*

Atomic displacement parameters (Å^2)

	U^{11}	U^{22}	U^{33}	U^{12}	U^{13}	U^{23}
Ca	0.0120 (3)	0.0142 (3)	0.0116 (3)	0.0024 (2)	0.0017 (2)	0.0017 (2)
V1	0.0140 (3)	0.0077 (2)	0.0094 (2)	0.00209 (19)	0.00032 (18)	0.00023 (18)
V2	0.0124 (2)	0.0082 (2)	0.0087 (2)	0.0026 (2)	−0.00078 (18)	−0.00002 (18)
O1	0.0216 (11)	0.0084 (10)	0.0098 (10)	0.0030 (9)	−0.0002 (8)	0.0005 (8)
O2	0.0116 (10)	0.0092 (10)	0.0109 (10)	0.0032 (8)	−0.0001 (8)	0.0002 (8)
OW3	0.0237 (13)	0.0201 (13)	0.0243 (14)	0.0026 (11)	0.0011 (10)	0.0030 (11)
O4	0.0131 (10)	0.0160 (11)	0.0162 (11)	0.0021 (9)	−0.0006 (8)	0.0013 (9)
O5	0.0211 (12)	0.0136 (11)	0.0232 (13)	0.0024 (9)	−0.0075 (9)	0.0003 (9)
O6	0.0347 (14)	0.0147 (11)	0.0204 (12)	0.0027 (11)	0.0151 (10)	0.0004 (9)
O7	0.0188 (11)	0.0170 (11)	0.0113 (10)	0.0064 (9)	0.0007 (8)	0.0020 (9)
OW8	0.0196 (13)	0.0132 (12)	0.0130 (11)	0.0005 (10)	−0.0014 (9)	0.0006 (9)

Geometric parameters (Å, º)

Ca—O7^i	2.381 (2)	V1—O1^{iii}	1.899 (2)
Ca—O4^{ii}	2.394 (2)	V1—O2	1.943 (2)
Ca—OW8^{ii}	2.441 (2)	V1—O1^{iv}	2.004 (2)
Ca—O6	2.448 (2)	V1—V1^v	3.1033 (10)
Ca—O2	2.476 (2)	V1—V2^{iv}	3.1187 (7)
Ca—O7	2.496 (2)	V2—O4	1.633 (2)

Ca—OW3	2.530 (3)	V2—O7	1.675 (2)
Ca—OW8^i	2.554 (2)	V2—O1	1.874 (2)
V1—O6	1.623 (2)	V2—O2	1.895 (2)
V1—O5	1.655 (2)	V2—O2^{iv}	2.075 (2)
O7^i—Ca—O4^{ii}	145.60 (8)	O6—Ca—OW8^i	71.80 (7)
O7^i—Ca—OW8^{ii}	79.03 (8)	O2—Ca—OW8^i	133.65 (7)
O4^{ii}—Ca—OW8^{ii}	84.88 (8)	O7—Ca—OW8^i	149.58 (7)
O7^i—Ca—O6	89.84 (8)	OW3—Ca—OW8^i	135.12 (8)
O4^{ii}—Ca—O6	88.49 (8)	O6—V1—O5	109.11 (13)
OW8^{ii}—Ca—O6	148.85 (8)	O6—V1—O1^{iii}	105.21 (11)
O7^i—Ca—O2	116.63 (7)	O5—V1—O1^{iii}	97.89 (11)
O4^{ii}—Ca—O2	93.49 (7)	O6—V1—O2	94.99 (10)
OW8^{ii}—Ca—O2	145.90 (8)	O5—V1—O2	97.89 (10)
O6—Ca—O2	64.79 (7)	O1^{iii}—V1—O2	148.57 (9)
O7^i—Ca—O7	72.07 (8)	O6—V1—O1^{iv}	114.83 (11)
O4^{ii}—Ca—O7	140.72 (7)	O5—V1—O1^{iv}	135.88 (11)
OW8^{ii}—Ca—O7	97.51 (8)	O1^{iii}—V1—O1^{iv}	74.72 (9)
O6—Ca—O7	106.65 (8)	O2—V1—O1^{iv}	75.01 (8)
O2—Ca—O7	63.17 (7)	O4—V2—O7	106.24 (11)
O7^i—Ca—OW3	131.12 (9)	O4—V2—O1	105.17 (10)
O4^{ii}—Ca—OW3	72.51 (9)	O7—V2—O1	100.84 (10)
OW8^{ii}—Ca—OW3	76.53 (8)	O4—V2—O2	106.81 (10)
O6—Ca—OW3	129.97 (8)	O7—V2—O2	93.48 (10)
O2—Ca—OW3	70.58 (8)	O1—V2—O2	139.47 (9)
O7—Ca—OW3	70.05 (8)	O4—V2—O2^{iv}	102.14 (10)
O7^i—Ca—OW8^i	77.53 (7)	O7—V2—O2^{iv}	151.38 (10)
O4^{ii}—Ca—OW8^i	69.34 (7)	O1—V2—O2^{iv}	74.79 (8)
OW8^{ii}—Ca—OW8^i	77.39 (8)	O2—V2—O2^{iv}	74.69 (9)

Symmetry codes: (i) −x+1, −y+1, −z; (ii) x+1, y, z; (iii) x, y−1, z; (iv) −x+1, −y+1, −z+1; (v) −x+1, −y, −z+1.

Hydrogen-bond geometry (Å, º)

D—H···A	D—H	H···A	D···A	D—H···A
OW3—H1···O4^{iv}	0.78 (5)	2.37 (5)	2.965 (4)	133 (4)
OW3—H2···O5^{vi}	0.72 (4)	2.25 (5)	2.900 (3)	150 (5)
OW8—H3···O5^{vii}	0.75 (4)	2.09 (5)	2.810 (3)	162 (5)
OW8—H4···O5^{viii}	0.84 (4)	1.97 (5)	2.794 (3)	166 (4)

Symmetry codes: (iv) −x+1, −y+1, −z+1; (vi) x+1, y+1, z; (vii) x, y+1, z; (viii) −x, −y+1, −z.